


Oviductal extracellular vesicles (oviductosomes, OVS) are conserved in humans: murine OVS play a pivotal role in sperm capacitation and fertility

Pradeepthi Bathala¹, Zeinab Fereshteh¹, Kun Li^{1,2},
Amal A. Al-Dossary^{1,3}, Deni S. Galileo¹,
and Patricia A. Martin-DeLeon^{1,*} 

¹Department of Biological Sciences, University of Delaware, Newark, DE 19716, USA ²Present address: Department of Reproductive Physiology, Zhejiang Academy of Medical Sciences, Room 205 B, Building 3, 182 Tian Mu Shan Road, Hangzhou, Zhejiang 310013, China ³Present address: Department of Biology, College of Medicine, University of Dammam (UOD), PO Box 2435, Dammam 31451, Saudi Arabia

*Correspondence address. 219 McKinly Lab, University of Delaware, Newark, DE 19716, USA. Tel: +1-302-831-2249; Fax: +1-302-831-2281; E-mail: pdeleon@udel.edu  orcid.org/0000-0002-6903-3703

Submitted on August 30, 2017; resubmitted on January 3, 2018; editorial decision on January 19, 2018; accepted on January 20, 2018

STUDY QUESTIONS: Are extracellular vesicles (EVs) in the murine oviduct (oviductosomes, OVS) conserved in humans and do they play a role in the fertility of *Pmca4*^{-/-} females?

SUMMARY ANSWER: OVS and their fertility-modulating proteins are conserved in humans, arise via the apocrine pathway, and mediate a compensatory upregulation of PMCA1 (plasma membrane Ca²⁺-ATPase 1) in *Pmca4*^{-/-} female mice during proestrus/estrus, to account for their fertility.

WHAT IS KNOWN ALREADY: Recently murine OVS were identified and shown during proestrus/estrus to express elevated levels of PMCA4 which they can deliver to sperm. PMCA4 is the major Ca²⁺ efflux pump in murine sperm and *Pmca4* deletion leads to loss of sperm motility and male infertility as there is no compensatory upregulation of the remaining Ca²⁺ pump, PMCA1. Of the four family members of PMCA (PMCA1–4), PMCA1 and PMCA4 are ubiquitous, and to date there have been no reports of one isoform being upregulated to compensate for another in any organ/tissue. Since *Pmca4*^{-/-} females are fertile, despite the abundant expression of PMCA4 in wild-type (WT) OVS, we propose that OVS serve a role of packaging and delivering to sperm elevated levels of PMCA1 in *Pmca4*^{-/-} during proestrus/estrus to compensate for PMCA4's absence.

STUDY DESIGN, SIZE, DURATION: Fallopian tubes from pre-menopausal women undergoing hysterectomy were used to study EVs in the luminal fluid. Oviducts from sexually mature WT mice were sectioned after perfusion fixation to detect EVs *in situ*. Oviducts were recovered from WT and *Pmca4*^{-/-} after hormonally induced estrus and sectioned for PMCA1 immunofluorescence (IF) (detected with confocal microscopy) and hematoxylin and eosin staining. Reproductive tissues, luminal fluids and EVs were recovered after induced estrus and after natural cycling for western blot analysis of PMCA1 and qRT-PCR of *Pmca1* to compare expression levels in WT and *Pmca4*^{-/-}. OVS, uterosomes, and epididymal luminal fluid were included in the comparisons. WT and *Pmca4*^{-/-} OVS were analyzed for the presence of known PMCA4 partners in sperm and their ability to interact with PMCA1, via co-immunoprecipitation. *In vitro* uptake of PMCA1 from OVS was analyzed in capacitated and uncapacitated sperm via quantitative western blot analysis, IF localization and flow cytometry. Caudal sperm were also assayed for uptake of tyrosine-phosphorylated proteins which were shown to be present in OVS. Finally, PMCA1 and PMCA4 in OVS and that delivered to sperm were assayed for enzymatic activity.

PARTICIPANTS/MATERIALS, SETTING, METHODS: Human fallopian tubes were flushed to recover luminal fluid which was processed for OVS via ultracentrifugation. Human OVS were negatively stained for transmission electron microscopy (TEM) and subjected to immunogold labeling, to detect PMCA4. Western analysis was used to detect HSC70 (an EV biomarker), PMCA1 and endothelial nitric oxide synthase (eNOS) which is a fertility-modulating protein delivered to human sperm by prostasomes. Oviducts of sexually mature female mice were sectioned after perfusion fixation for TEM tomography to obtain 3D information and to distinguish cross-sections of EVs from those of microvilli and cilia. Murine tissues, luminal fluids and EVs were assayed for PMCA1 (IF and western blot) or qRT-PCR. PMCA1 levels from

western blots were quantified, using band densities and compared in WT and *Pmca4*^{-/-} after induced estrus and in proestrus/estrus and metestrus/diestrus in cycling females. *In vitro* uptake of PMCAI and tyrosine-phosphorylated proteins was quantified with flow cytometry and/or quantitative western blot. Ca²⁺-ATPase activity in OVS and sperm before and after PMCAI and PMCA4 uptake was assayed, via the enzymatic hydrolysis rate of ATP.

MAIN RESULTS AND THE ROLE OF CHANCE: TEM revealed that human oviducts contain EVs (exosomal and microvesicular). These EVs contain PMCA4 (immunolabeling), eNOS and PMCAI (western blot) in their cargo. TEM tomography showed the murine oviduct with EV-containing blebs which typify the apocrine pathway for EV biogenesis. Western blots revealed that during proestrus/estrus PMCAI was significantly elevated in the oviductal luminal fluid (OLF) ($P = 0.02$) and in OVS ($P = 0.03$) of *Pmca4*^{-/-}, compared to WT. Further, while PMCAI levels did not fluctuate in OLF during the cycle in WT, they were significantly ($P = 0.02$) higher in proestrus/estrus than at metestrus/diestrus in *Pmca4*^{-/-}. The elevated levels of PMCAI in proestrus/estrus, which mimics PMCA4 in WT, is OLF/OVS-specific, and is not seen in oviductal tissues, uterosomes or epididymal luminal fluid of *Pmca4*^{-/-}. However, qRT-PCR revealed significantly elevated levels of *PmcaI* transcript in *Pmca4*^{-/-} oviductal tissues, compared to WT. PMCAI could be transferred from OVS to sperm and the levels were significantly higher for capacitated vs uncapacitated sperm, as assessed by flow cytometry ($P = 0.001$) after 3 h co-incubation, quantitative western blot ($P < 0.05$) and the frequency of immuno-labeled sperm ($P < 0.001$) after 30 min co-incubation. Tyrosine phosphorylated proteins were discovered in murine OVS and could be delivered to sperm after their co-incubation with OVS, as detected by western, immunofluorescence localization, and flow cytometry. PMCAI and PMCA4 in OVS were shown to be enzymatically active and this activity increased in sperm after OVS interaction.

LARGE SCALE DATA: None.

LIMITATIONS REASONS FOR CAUTION: Although oviductal tissues of WT and *Pmca4*^{-/-} showed no significant difference in PMCAI levels, *Pmca4*^{-/-} levels of OVS/OLF during proestrus/estrus were significantly higher than in WT. We have attributed this enrichment or upregulation of PMCAI in *Pmca4*^{-/-} partly to selective packaging in OVS to compensate for the lack of PMCA4. However, in the absence of a difference between WT and *Pmca4*^{-/-} in the PMCAI levels in oviductal tissues as a whole, we cannot rule out significantly higher PMCAI expression in the oviductal epithelium that gives rise to the OVS as significantly higher *PmcaI* transcripts were detected in *Pmca4*^{-/-}.

WIDER IMPLICATIONS OF THE FINDINGS: Since OVS and fertility-modulating cargo components are conserved in humans, it suggests that murine OVS role in regulating the expression of proteins required for capacitation and fertility is also conserved. Secondly, OVS may explain some of the differences in *in vivo* and *in vitro* fertilization for mouse mutants, as seen in mice lacking the gene for FER which is the enzyme required for sperm protein tyrosine phosphorylation. Our observation that murine OVS carry and can modulate sperm protein tyrosine phosphorylation by delivering them to sperm provides an explanation for the *in vivo* fertility of *Fer* mutants, not seen *in vitro*. Finally, our findings have implications for infertility treatment and exosome therapeutics.

STUDY FUNDING AND COMPETING INTEREST(S): The work was supported by National Institute of Health (RO3HD073523 and 5P20RR015588) grants to P.A.M.-D. There are no conflicts of interests.

Key words: exosomes / capacitation / sperm tyrosine phosphorylation / PMCAI / Ca²⁺ efflux pumps / human oviductosomes / *Pmca4* null female

Introduction

Extracellular vesicles (EVs) are nano-sized spherical membrane-bound vesicles released in biofluids from cell membranes and are known to mediate intercellular communication, and thus play important roles in physiological and pathophysiological processes (Simons and Raposo, 2009; Thery et al., 2009). There is evidence that EVs play essential roles in the male reproductive tract, as in the epididymal luminal fluid and the prostatic fluid epididymosomes and prostasomes relay complex macromolecular cargoes to sperm to facilitate their functional transformation (Machtinger et al., 2016; Martin-DeLeon, 2016). Plasma membrane Ca²⁺-ATPase 4 (PMCA4) is a testicular/sperm protein that is also expressed in human prostasomes which can transfer it to sperm *in vitro* (Andrews et al., 2015). In mice PMCA4 is delivered to sperm by epididymosomes (Patel et al., 2013), is the major Ca²⁺ efflux pump (Wennemuth et al., 2003), and is likely to be stimulated by the decapacitation factor that prevents premature capacitation (Adeoya-Osiguwa and Fraser, 1996). Capacitation is the final maturation process that sperm undergo in the female before they are

competent to undergo the acrosome reaction and effect fertilization (Austin, 1952; Chang, 1955).

More recently, in mice EVs were identified in the uterine and oviductal fluids where they are referred to as uterosomes (Griffiths et al., 2008) and oviductosomes (Griffiths et al., 2008; Al-Dossary et al., 2013). These were shown to express essential sperm proteins as sperm adhesion molecule I (SPAM1) and PMCA4 in elevated levels during proestrus/estrus, but only marginal levels during metestrus/diestrus (Griffiths et al., 2008; Al-Dossary et al., 2013) when females do not mate. Further, these EVs were able to deliver these fertility-modulating proteins to sperm *in vitro* (Griffiths et al., 2008; Al-Dossary et al., 2013). Cargo delivery from oviductosomes (OVS) to sperm was shown to occur via a fusogenic mechanism mediated by integrins (Al-Dossary et al., 2015). Delivery of PMCA4 to sperm could not only prevent premature capacitation by keeping intracellular Ca²⁺ low (Adeoya-Osiguwa and Fraser, 1996), but might also facilitate a return to homeostatic Ca²⁺ levels following the Ca²⁺ fluxes required for capacitation and the acrosome reaction (Al-Dossary et al., 2013).

The importance of PMCA4 as an essential Ca^{2+} efflux mechanism in sperm is underscored by the finding that its targeted deletion in mice leads to intracellular Ca^{2+} overload, loss of sperm motility and male infertility (Okunade *et al.*, 2004; Schuh *et al.*, 2004). While PMCA4 predominates in sperm, accounting for >90% of PMCAs, the PMCA1 isoform, which is also ubiquitously expressed (Strehler *et al.*, 2007) accounts for the remaining 10% (Okunade *et al.*, 2004). Notably, in *Pmca4*^{-/-} males the expression of PMCA1 is unaltered relative to that in wild-type (WT) (Okunade *et al.*, 2004), leading to Ca^{2+} toxicity which has been shown to mediate the loss of sperm motility and to result in oxidative stress (Olli *et al.*, 2018). It should be noted that, to date, there are no examples of one PMCA isoform compensating for loss of another.

Pmca4^{-/-} females, unlike males, are surprisingly fertile (Okunade *et al.*, 2004; Schuh *et al.*, 2004), despite the abundant expression of PMCA4 in the WT female tract, particularly in OVS from which it is delivered to sperm *in vitro* (Al-Dossary *et al.*, 2013, 2015). Thus adequate Ca^{2+} efflux mechanisms in *Pmca4*^{-/-} oviduct would be expected to be in place to maintain not only Ca^{2+} homeostasis of sperm in the oviduct, but also normal ciliary function of the oviductal epithelium that is required for oocyte transport (Ghersevich *et al.*, 2015). Based on the above, we hypothesize that in the absence of potential compensatory synthesis of PMCA1 in *Pmca4*^{-/-} oviduct, OVS modulate PMCA1's expression such that it acts as a true surrogate for oviductosomal PMCA4, with respect to its abundance in proestrus/estrus. Thus, female fertility is maintained.

Our findings show that while the levels of *Pmca1* transcript are significantly elevated in KO, compared to WT oviduct; PMCA1 levels are not significantly different. The data therefore support our hypothesis and highlight the critical role of OVS in regulating female fertility. Additionally, we provide, for the first time, evidence for the biogenesis of OVS via the apocrine pathway, for their evolutionary conservation in humans (where their cargo includes both PMCA4 and PMCA1), and for their delivery of enzymatically active PMCAs and tyrosine phosphorylated proteins to sperm. The selective enrichment of PMCA1 in *Pmca4*^{-/-} OVS during proestrus/estrus coupled with enhancement of protein tyrosine phosphorylation (a key capacitation event) after sperm–OVS interaction, provides strong evidence for the pivotal role of OVS in regulating female fertility.

Materials and Methods

Ethical approval

The studies were approved by the Institutional Animal Care and Use Committee at the University of Delaware and were in agreement with the Guide for the Care and Use of Laboratory Animals published by the National Research Council of the National Academies, 8th ed., Washington, DC (publication 85–23, revised 2011).

Mice and reagents

Sexually mature 10–12-week-old males and 4–12-week-old female mice (FVB/N strain; Harlan, Indianapolis, IN) were used for this study. Additionally, *Pmca4*^{-/-} males and females on the FVB/N background were used to obtain testis and oviductal tissues, and uterine, and epididymal luminal fluids, OVS and uterosomes for western blotting. These mutant mice, generated in the laboratory of Dr Gary Shull (University of Cincinnati), were a generous gift. They were bred and genotyped as described previously (Okunade *et al.*, 2004). All enzymes and chemicals were purchased from Fisher Scientific Co.

(Malvern, PA), Sigma (St Louis, MO) or Invitrogen (Carlsbad, CA), unless otherwise specified.

Human fallopian tubes

Normal Fallopian tubes were obtained from two pre-menopausal women (35 and 40 years old) at the time of hysterectomy, through the National Disease Research Interchange (Philadelphia, PA). One was frozen and the other received in medium within 24 h post-surgery.

Antibodies

Rabbit monoclonal anti-PMCA1 antibody (ab190355) and the IgG isotype control (ab172730) were purchased from Abcam (Cambridge, MA) and used for immunofluorescence (IF), western blots and flow cytometric studies. Mouse monoclonal anti-HSC70 antibody (sc-7298), goat polyclonal anti-PMCA4 antibody (SC-22 080), rabbit polyclonal nNOS antibody (NOS1), rabbit polyclonal eNOS antibody (NOS3) and anti-phosphotyrosine antibody (PY99) a mouse monoclonal antibody (sc-7020) were purchased from Santa Cruz Biotechnology (Dallas, TX). Also, mouse monoclonal anti-phosphotyrosine antibody (clone 4G10) was obtained from Millipore (Temecula, CA). β -actin antibody (A5316), a mouse monoclonal, was obtained from Sigma. Mouse monoclonal anti-CASK antibody (#75-000) was obtained from UC Davis/NINDS/NIMH NeuroMab Facility (Davis, CA). Secondary antibodies were purchased from Santa Cruz Biotech, Inc., Life Technologies or Molecular Probes Inc. (Eugene, OR). Fluoro-Gel II with DAPI (17 985-50), for IF, was obtained from Electron Microscope Sciences (Hatfield, PA).

Perfusion of mice for oviductal sectioning

The lumen of the oviducts of sexually mature females were flushed in a glutaraldehyde/formaldehyde perfusate (1% each in phosphate buffered saline (PBS)) immediately after sacrifice, and fixed in 2% glutaraldehyde and 2% formaldehyde in 0.1 M sodium cacodylate buffer pH 7.4 containing 2 mM calcium chloride. The tissue was cut into 1–2 mm³ pieces. Samples were sectioned on a Reichert-Jung Ultracut E ultramicrotome, and sections collected onto 200 mesh formvar-carbon coated copper grids and post-stained with 2% uranyl acetate in 50% methanol and Reynolds lead citrate (Reynolds, 1963). For tomography, sections were cut to 250 nm thickness and 20 and 50 nm colloidal gold was adsorbed to each side of the grid to serve as fiducial markers for tomographic alignment. Dual-axis tilt series were acquired on a Zeiss Libra 120 transmission electron microscope, using a Gatan Ultrascan 1000 CCD. Tilt series were collected from –65° to +65° and images were acquired at 1° increments. Tomograms were generated with IMOD (Kremer *et al.*, 1996), using an R-weighted back-projection algorithm.

Superovulation of female mice

To hormonally induce estrus, 4–6-week-old females were sequentially injected with pregnant mare serum gonadotropin (PMSG, 7.5 i.u.) and HCG (7.5 i.u.), 48 h apart. After 13.5–14 h from the last injection, females were sacrificed and their reproductive tissues collected for analysis.

Identification of the stages of the murine estrus cycle

The stages of the estrus cycle of 8–12-week-old virgins were classified based on the proportion of different cell types identified in the vaginal secretion (Byers *et al.*, 2012). Based on PMCA4 expression (Al-Dossary *et al.*, 2013), oviductal tissues at proestrus/estrus were pooled, similar to metestrus/diestrus, and processed for analysis as described below.

Collection of female reproductive tissues, luminal fluids and EVs

Immediately after sacrificing, oviducts and uteri were removed. Luminal fluids were collected in PBS with protease inhibitors after mincing the oviducts or flushing the uteri as previously described (Griffiths et al., 2008; Al-Dossary et al., 2013). These luminal fluids were clarified by centrifugation at 3500 g for 10 min to exclude cells and tissue fragments, and then frozen immediately at -80°C for further processing. Following this, clarified oviductal luminal fluid (OLF) and uterine luminal fluid (ULF) were subjected to ultracentrifugation at 120 000 g at 4°C for 2 h using Beckman Optima 2–70 k ultracentrifuge and a Ti60 rotor, as described (Griffiths et al., 2008). Resulting pellets (OVS and uterosomes) were separately re-suspended in homogenization buffer with protease inhibitor for western blotting.

EVs were collected from human fallopian tubes by flushing the lumens with PBS. The lavage was clarified by centrifugation and subjected to ultracentrifugation, as described above. The pellets were re-suspended in PBS for transmission electron microscopy (TEM) or in a homogenization buffer and protease inhibitor for western blot analysis.

Negative staining for TEM and immunogold labeling of PMCA4 on human EVs

Nickel TEM grids (Electron Microscopy Sciences, Hatfield, PA, USA), 400 mesh with a formvar/carbon film, were floated on a drop of the pellet suspension from the purified human Fallopian tube fluid. The grids were then washed with several drops of water and stained with 1% uranyl acetate, a phospholipid stain, before being subjected to microscopic analysis. Membrane vesicles were imaged using a Zeiss LIBRA 120 (Germany) for TEM. Immunogold labeling was performed as previously described using anti-PMCA4 primary antibodies (Al-Dossary et al., 2013).

Preparation of capacitated sperm

Murine sperm were collected by mincing caudal epididymides of sexually mature males in human tubal fluid (HTF) (Cat #2005, InVitroCare, Frederick, MD), a capacitation medium. Minced tissue was left at 37°C for 10 min for sperm to swim out (Chen et al., 2006). After gravity settling of tissues, the supernatant was centrifuged (500 g, 15 min) and aliquoted to be used immediately as uncapacitated sperm or to be incubated in fresh HTF at 37°C for 90 min for capacitation.

Indirect IF staining

Oviductal, uterine and vaginal tissues collected from superovulated females were embedded immediately in optimal cutting temperature (OCT) medium (Tissue Tek, Torrance, CA) and frozen at -80°C . Cryostat sections (20 μm) were made and slides fixed in pre-chilled 1:1 acetone:methanol at -20°C for 20 min and air-dried for 10 min before being placed in blocking solution (1% bovine serum albumin (BSA) in PBS) for 2 h at RT. Slides were then incubated in anti-PMCA1 primary antibody or rabbit IgG (negative control) at a dilution of 1:50 in blocking solution, overnight in an enclosed humid chamber. Following this, slides were washed with PBS (2 \times , 20 min) and incubated in Alexa Fluor 568-conjugated goat anti-rabbit IgG (Molecular Probes, Eugene OR) at a dilution of 1:200 in blocking solution for 45 min at RT in the dark, followed by washing with PBS (2 \times , 20 min). Finally, sections were mounted with Fluoro gel II mounting media with DAPI and coverslipped. Slides were visualized, using a Zeiss LSM 780 confocal microscope (Carl Zeiss, Inc, Gottingen, Germany).

Preparation of total RNA and real-time RT-PCR

Total RNA was extracted from pooled frozen WT and KO oviductal tissues using the miRCURY™ RNA Isolation Kit (#300110, Exiqon, MA, USA), according to the manufacturer's protocol. cDNA was synthesized using the iScript cDNA Synthesis Kit (#1708890, Bio-Rad, CA, USA). Total RNA (500 ng) from each sample was reverse transcribed at 42°C for 30 min followed by inactivation at 85°C for 5 min. qPCR was performed using Power SYBR Green PCR Master Mix (Invitrogen) in the QuantStudio 6 Flex Real-Time PCR System (Applied Biosystems). Reactions, including non-template controls, were set up and experiments were run in triplicate. For *Pmca1* two pairs of primers were used: (i) forward (5'-GCTCTGTGATGACTGGCAA-3') and reverse (5'-TCTCTTCCCCACAGCACTCT-3') primers designed by the Primer3 program (Rozen and Skaletsky, 2000) amplified a 236 bp product, and (ii) forward (5'-GTGAGACACCTGGACGCTTGAGACC-3') and reverse (5'-TCCCCGTTACCAGGTAGGACAGGA-3') primers amplified a 183-bp product (Okunade et al., 2004). For *Gapdh*, an endogenous reference control, forward (5'-CCGCATCTTCTTGTGCAGT-3') and reverse (5'-GAATTTGCCCGTGAGTGGAGT-3') primers amplified a 204 bp product. Data for each sample were normalized against the level of *Gapdh*. The relative expression of transcripts in samples were analyzed using the comparative Ct ($\Delta\Delta\text{Ct}$) method. The RT-PCR products were electrophoresed on 2% agarose gel stained with ethidium bromide and run in Tris-acetate-EDTA (TAE) buffer.

Sodium dodecyl sulfate-polyacrylamide gel electrophoresis (SDS-PAGE) and western blot analysis

Protein extracts of female tissues, testis or EVs were prepared as mentioned previously. Samples for electrophoresis were diluted in 5 \times Laemmli sample buffer and heated at 99°C for 5 min. The 20–40 μg of proteins (or as specified) from tissues, fluids or OVS were loaded on each lane of 10% polyacrylamide gels and transferred onto nitrocellulose membrane (Amersham Biosciences, UK). Blots were blocked for 1 h at RT, incubated in anti-PMCA1 (1:2000) primary antibody [or anti-CASK (1:1000), or anti-nNOS (1:500), anti-HSC70 (1:1000), anti-PY (1:200)] overnight at 4°C , and processed as previously described (Al-Dossary et al., 2013). Membranes were re-probed with HSC70 antibody, which served as an internal loading control for normalization and as an EV biomarker. The normalization approach was as described (<http://bitesizebio.com/23411/the-4-important-steps-for-western-blot-quantification/>). To quantify the intensity of the bands, images from shorter film exposures were selected and Image J software (Rasband, 1997–2016) was used to subtract the background from the PMCA1 band and that of the HSC70 loading control.

Co-immunoprecipitation of PMCA1 and interacting partners in OLF

Co-immunoprecipitation assays were performed as previously described (Aravindan et al., 2012; Olli et al., 2018), using PureProteome Protein G magnetic beads (Millipore Corp, Billerica, MA) which were washed with PBS and treated with 2 μg of specific antibody (nNOS or CASK) for 2 h on rotator at 4°C . Control beads were treated with the same concentration of either rabbit or mouse IgG. After incubation, the beads were washed, re-suspended in OLF (500 μg protein) in immunoprecipitation buffer (25 mM Tris, 150 mM NaCl, pH 7.2) and protease inhibitor for a total of 500 μl , and incubated on a rotator at 4°C overnight. Following incubation, beads were washed and the proteins eluted and processed for western blotting as described (Aravindan et al., 2012; Olli et al., 2018).

In vitro sperm uptake of PMCAI and tyrosine-phosphorylated proteins from OVS

Aliquots of uncapacitated and capacitated sperm were co-incubated with OLF/OVS, PBS or the supernatant (SUP) after OVS isolation for 30 min or 3 h at 37°C and assayed for PMCAI uptake as previously described (Al-Dossary *et al.*, 2013, 2015), except that uptake was also assessed by quantitative western blotting and localization of IF. Alternatively, sperm were co-incubated in PBS, HTF or OVS for 30 min, 90 min and 3 h before quantification of PMCAI uptake. For tyrosine-phosphorylated proteins, sperm aliquots were co-incubated with PBS, HTF and OVS re-constituted in PBS for 2 h. After co-incubation, sperm were washed with PBS and fixed in 1.5% paraformaldehyde for 1 h at RT. After washing they were permeabilized with 0.1% triton X-100 for 10 min at RT. They were then washed with PBS and blocked with 2% BSA and treated with the primary antibodies diluted 1:200 for anti-PMCAI and 1:50 for anti-phosphotyrosine followed by the appropriate secondary antibodies conjugated to Alexa Fluor 488. Uptake was quantified using a FACSCalibur or a FACSAria™ II (BD Sciences, San Jose, CA), flow cytometer equipped with an argon laser with excitation at 488 nm.

Mg²⁺-dependent Ca²⁺-ATPase activity in OVS and sperm

Ca²⁺-ATPase activity was performed as previously performed in our Lab (Kosk-Kosicka, 1999; Post *et al.*, 2010; Aravindan *et al.*, 2012). Briefly, total membranes were prepared from capacitated sperm and OVS after homogenization and centrifugation (4 000 g, 10 min, 4°C). The supernatant was ultracentrifuged (100 000 g, 60 min, 4°C) to yield microsomes in the pellet which was re-suspended for 15 min in 100 µl homogenization buffer containing 1.5% *n*-octyl-β-glucopyranoside, and the protein concentration determined with the biocinchoninic acid (BCA) kit (Pierce, Rockford, IL). The reaction mixture was as described (Kosk-Kosicka, 1999), with the addition of 2 µg/ml oligomycin, a specific blocker of mitochondrial ATPases, added to the reaction buffer. The enzymatic hydrolysis rate of ATP was determined via quantification of the resulting inorganic phosphate (P_i) as a function of time. The assay was performed at 37°C for 30 min using 5 µg of microsomal proteins and 60 mM ATP. Duplicate reactions were terminated with Lin-Morales reagent and the P_i measured colorimetrically as a complex of molybdoanadate, using a spectrophotometer with absorbance at 350 nm. Absorbance was converted into P_i using a calibration curve of known concentrations of K₂HPO₄. Experiments were performed in triplicate and the mean activity expressed as µmol/P_i/mg protein/h.

Statistical analysis

Experiments were performed at least three times and the means (± SEM) of the normalized data for band density analyzed using Student's *t*-tests, one-way and two-way ANOVA. Chi-squared (χ²) analysis with Yates' correction was used for frequency distribution. Differences were considered to be significant when **P* < 0.05, ***P* < 0.01, ****P* < 0.001, *****P* < 0.0001.

Results

Human fallopian tubal fluid contains EVs which carry PMCAI and eNOS in their cargo

OVS were detected in the secretion of human Fallopian tubes, for the first time. TEM revealed that they consist of both microvesicles and exosomes (Fig. 1A (a)), ranging from 50 to 250 nm in diameter. Immunogold labeling for the detection of PMCA4 showed OVS with a positive signal (Fig. 1A (b, c)), compared to the IgG control where gold

particles were seen only in the background (Fig. 1A (a)). Western analysis showed human OVS to contain heat shock cognate 70 protein (HSC70) (Fig. 1B and C), a notable biochemical marker of EVs, validating their identity. PMCAI (Fig. 1B) and endothelial nitric oxide synthase (eNOS) (Fig. 1C), a fertility-modulating sperm protein (Olli *et al.*, 2018), were also detected in human OVS.

EVs in the murine oviduct arise via the apocrine pathway

With perfusion fixation of the murine oviduct and TEM of tissue sections, we detected OVS *in situ* (both microvesicles and exosomes) in blebs that were dislodged in the lumen (Fig. 2A). These OVS-containing blebs are distinguishable from cross-sections of microvilli and cilia by their pleomorphic nature. TEM tomography (Fig. 2B)

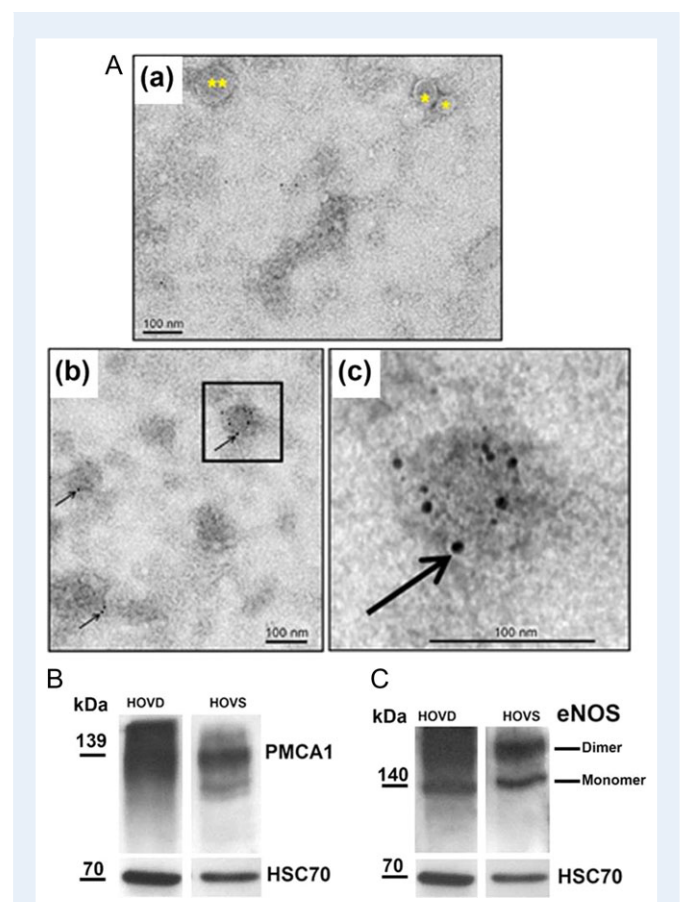


Figure 1 Oviductosomes (OVS) are evolutionarily conserved in humans and carry PMCAI. **(A)** TEM of negatively stained human OVS showing immunogold labeling of PMCA4. (a) The IgG control shows a microvesicle (**), larger OVS (0.1–1 µm) and an exosome (*) < 100 nm. (b) Immunogold labeling (6 nm gold particles) of PMCA4 (arrows) showing gold particles on OVS. These particles are seen only on the background in (a). The inset in (b) is enlarged in (c) to show the particles (bar = 100 nm). **(B, C)** Western blots show the presence of HSC70, an extracellular vesicle (EV) biochemical marker, after stripping of the membrane, as well as PMCAI and eNOS (in dimeric and monomeric forms) in human OVS (HOVS) and human oviductal tissues (HOVD).

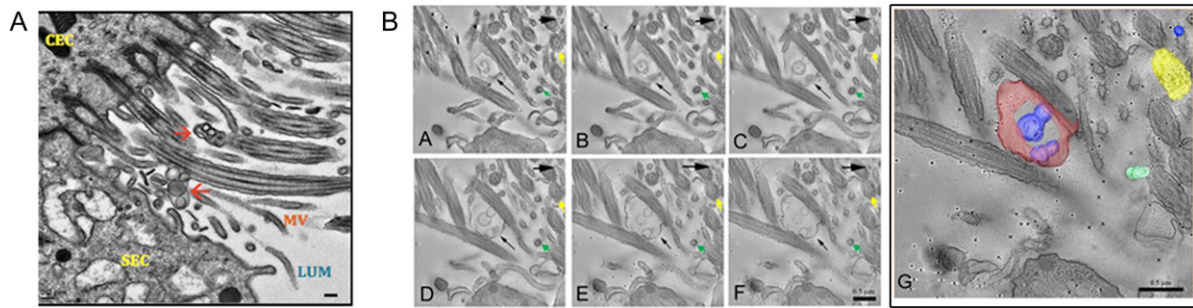


Figure 2 OVS arise from the apocrine pathway. **(A)** TEM of murine oviductal epithelium. Red arrows show blebs, containing OVS, in the lumen (LUM) among sections of cilia from the ciliated cells (CEC) and microvilli (MV) of the secretory cells (SEC). Blebs are typically found when EVs arise via the apocrine pathway (bar = 0.2 μ m). **(B)** TEM tomographic series reveals OVS arising from the apocrine pathway. Small black arrows show different planes (B (A–F)) of an OVS-containing bleb, released from the epithelium. Large black arrows show different planes of the 3D structure of an EV, not seen for microvilli (green arrow) or cilia (yellow arrow). **(G)** An enlarged 3D surface rendering overlaid on the last slide (B (F)) of the tomogram with the bleb (containing blue EVs) seen in red, an isolated exosome (blue) is at the top right, microvilli (green) and a cilium (yellow) are seen (bar = 0.5 μ m).

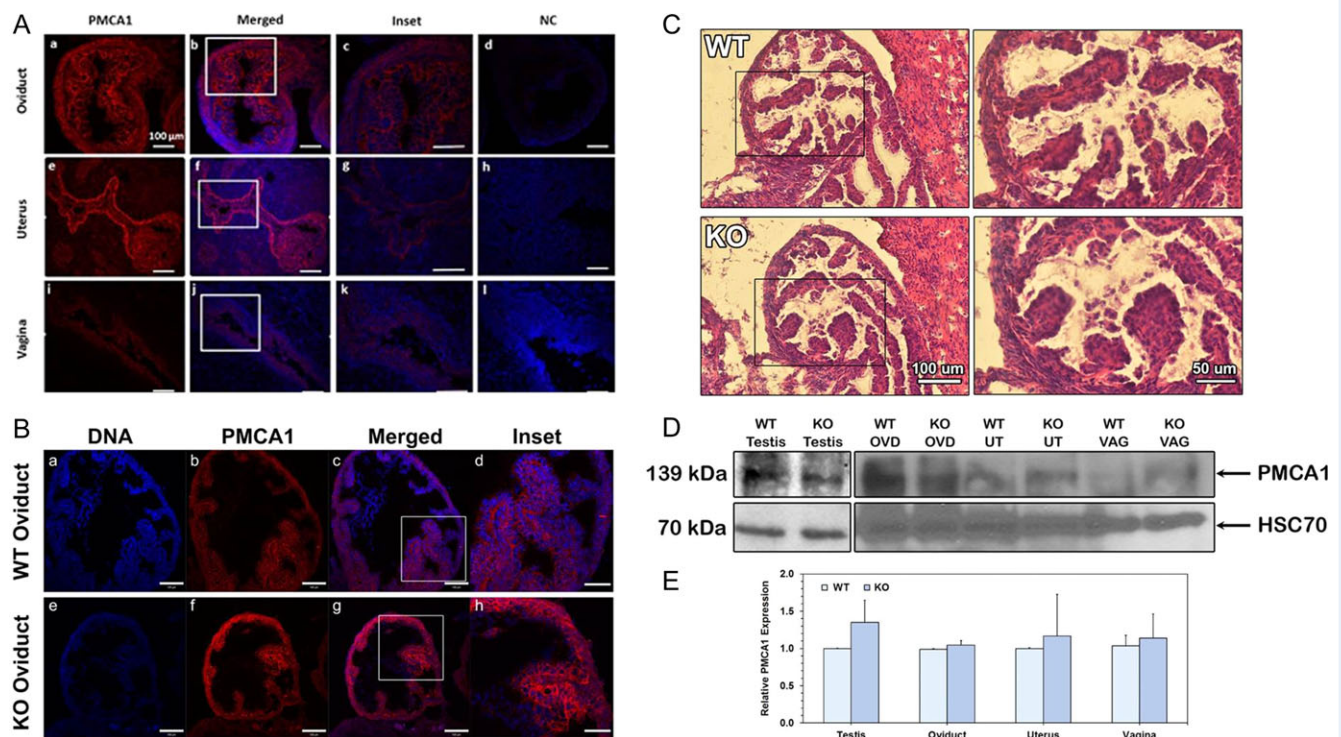


Figure 3 PMCA1 expression levels in murine reproductive tissues during estrus show no difference in WT and *Pmca4* KO oviducts. **(A)** Indirect immunofluorescence shows a strong PMCA1 signal (red) in the oviduct and uterus throughout, including both the apical and basement membranes. A weaker signal is seen in the vagina. Insets are shown in A (c, g and k). Negative controls (NC; rabbit IgG) do not show the staining (d, h and i) and validate the specificity of the PMCA1 antibody. **(B)** PMCA1 staining shows no difference in intensity of the signal between *Pmca4* KO (f) and WT (b) oviduct. Enlarged images are seen in the insets (d and h) and the DNA staining is blue. Bar = 100 μ m (200 μ m for all insets and the same scale for all micrographs). **(C)** Hematoxylin and eosin staining of oviductal sections shows no difference in histology between WT and KO. **(D)** Representative western blot of estrus tissue lysates showed the 139 kDa PMCA1, with testis as a positive control. The membrane was stripped and re-probed with HSC70, as a loading control. **(E)** Quantification of western blot data in (D) represents the mean (\pm SEM, $n = 3$) of band intensities, using Image Lab 6.0 software. Statistical analysis showed no difference between WT and KO tissues.

provided a 3D picture of the bleb and also the spherical nature of OVS, confirming their existence *in situ*. OVS are distinguishable from cilia, which contain microtubules, and from microvilli which are smaller. The 3D structures of a bleb with OVS, revealed by TEM tomography, show changes in the different planes (A–F), not seen for microvilli (green arrow) and cilia (yellow arrow) (Fig. 2B). The red-staining bleb in Fig. 2B (G) is a 3D rendering of (A–F) in Fig. 2B. Thus, tomography reveals that OVS arise via the apocrine pathway, as typified by the presence of blebs which release their EVs into the lumen.

Localization and expression analysis of PMCA1 in murine female reproductive tissues

Indirect IF and confocal microscopy of oviductal, uterine, and vaginal tissues of WT superovulated virgins revealed that PMCA1 is expressed in all three organs (Fig. 3A). Compared to that of the vagina, the luminal epithelial cells and basement membrane of the oviduct and the uterus show a stronger PMCA1 signal which was seen throughout the tissue, including the basement membranes (Fig. 3A). Oviductal sections from superovulated WT and *Pmca4*^{-/-} (KO) reveal that PMCA1 is present in the apical and basement membranes (Fig. 3B), while hematoxylin and eosin staining showed the histology to be similar in both (Fig. 3C). The occurrence of PMCA1 in the apical membranes of the epithelia suggests that PMCA1 is secreted into the oviductal fluids via EVs.

In order to corroborate the indirect IF findings for PMCA1, western blot analysis was performed on tissue lysates of superovulated females. In all the lysates of WT and *Pmca4*^{-/-} oviduct, uterus, and vagina a 139 kDa PMCA1 band was detected (Fig. 3D), confirming the indirect IF data. Western also revealed that PMCA1 expression levels varied, although there was no significant difference ($P > 0.05$) between WT and *Pmca4*^{-/-} female or testicular tissue, used as a positive control (Fig. 3E).

Elevated levels of PMCA1 are present in the oviductal secretion

OLF collected from WT and *Pmca4* KO females in hormonally induced estrus was assayed for the presence of PMCA1, using western blot analysis. Figure 4A shows that PMCA1 is present in WT and *Pmca4* KO OLF as well as epididymal luminal fluid (ELF), used as a positive control. The intensity of the bands revealed that the expression of PMCA1 varied with the phenotype: in hormonally induced estrus there was an insignificant ($P = 0.07$) increase of PMCA1 in *Pmca4* KO OLF compared to WT, not seen for ELF (Fig. 4B). However, OLF collected during proestrus/estrus from naturally cycling females had significantly ($P = 0.02$) higher levels of PMCA1 in *Pmca4*^{-/-} compared to WT (Fig. 4C and D). Furthermore, in *Pmca4*^{-/-} the levels of PMCA1 in OLF at metestrus/diestrus and proestrus/estrus were significantly different ($P = 0.02$) while they were not for the WT ($P = 0.1$) (Fig. 4D).

PMCA1 is significantly elevated in estrus OVS but not in uterosomes

Using testis as a positive control, proteins in OVS and uterosomes of WT and *Pmca4*^{-/-} females induced into estrus were subjected to western blot analysis. Both showed the 139 kDa PMCA1 (Fig. 5A)

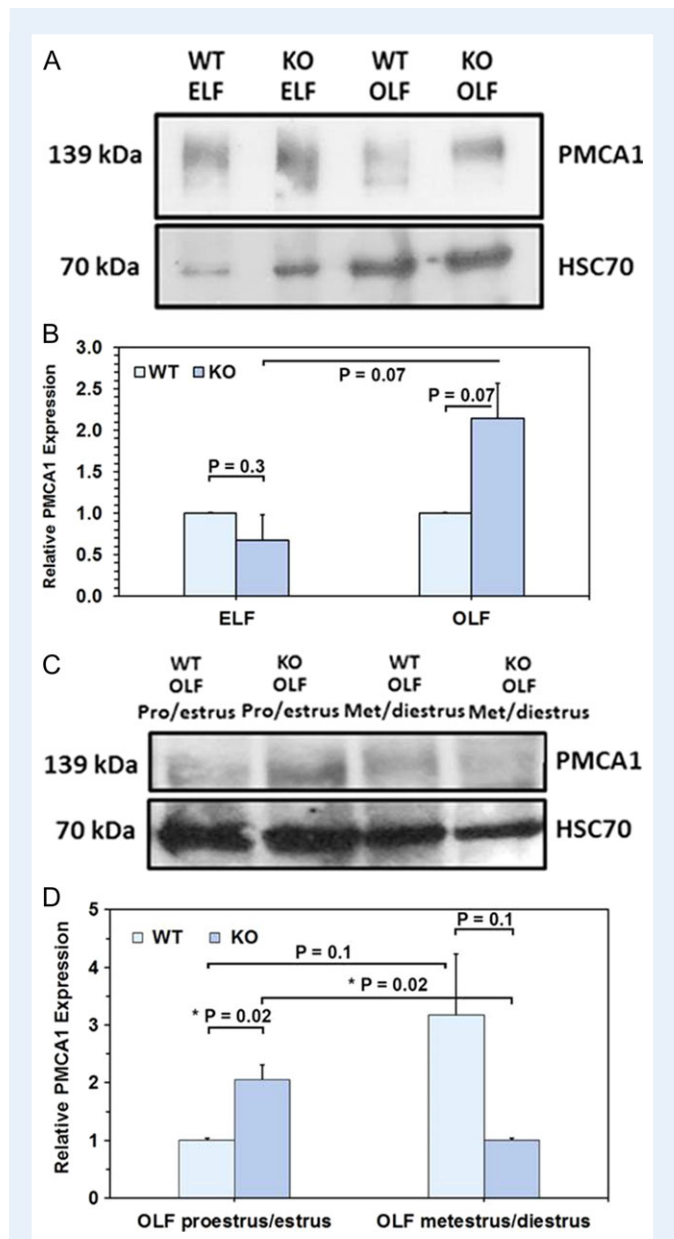


Figure 4 Oviductal luminal fluid (OLF) of WT and *Pmca4* KO shows elevated levels of PMCA1 in estrus during natural cycling in KO only. (A, B) Western blot of WT and KO OLF after hormonally induced estrus of PMCA1 in *Pmca4* KO, compared to WT ($P = 0.07$, $n = 3$). Epididymal luminal fluids from *Pmca4* KO and WT were included and showed no difference ($P = 0.1$, $n = 3$). (C, D) *Pmca4* KO OLF shows a significant ($*P = 0.02$) increase during proestrus/estrus vs WT OLF and a significant decrease ($*P = 0.02$) during metestrus/diestrus of PMCA1, using One-way ANOVA and Student *t*-tests.

whose intensity reflected an upregulation in OVS of *Pmca4*^{-/-}, compared to WT, while similar levels were detected in WT and *Pmca4*^{-/-} uterosomes (Fig. 5C and D). Band intensity of the OVS PMCA1 revealed a significant ($P = 0.03$) 13-fold PMCA1 increase in *Pmca4*^{-/-}, compared to WT (Fig. 5B). Real-Time PCR quantification of *Pmca1* mRNA showed significantly higher ($P = 0.02$) expression levels of

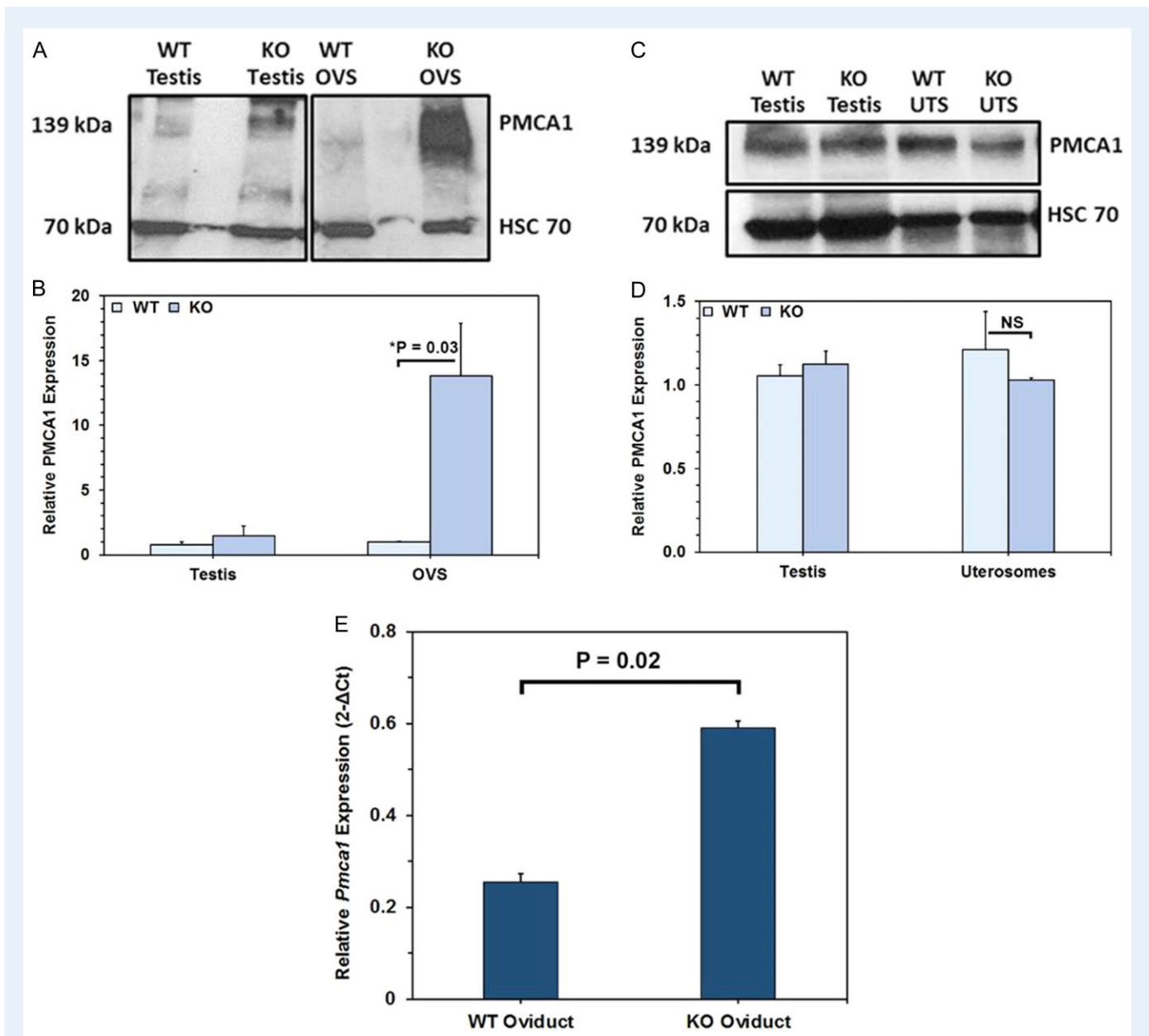


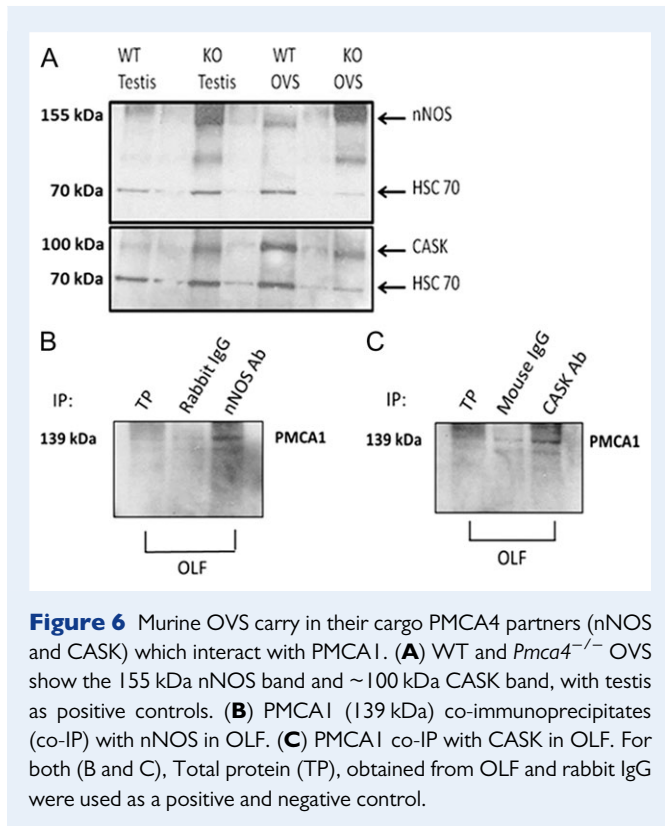
Figure 5 Compared to WT, estrus *Pmca4*^{-/-} OVS (unlike uterosomes) and oviductal tissues have significantly elevated PMCA1 and *Pmca1* mRNA levels, respectively. Representative Western of PMCA1 in OVS (A) and uterosomes (C) of WT and *Pmca4* KO females, with the HSC70 loading controls, and testis used as positive control. (B) Student *t*-tests ($n = 3$) show a significant increase (* $P = 0.03$) of PMCA1 in *Pmca4* KO, compared to WT OVS, but not in uterosomes (D). (E) *Pmca1* mRNA in oviductal tissues normalized to *Gapdh* ($n = 3$) shows a significant increase ($P = 0.02$) in *Pmca4*^{-/-}, compared to WT. Similar results were seen for both pairs of primer. Agarose gel electrophoresis of the RT-PCR products are shown in Supplemental Fig. S1.

transcripts in pro/estrus oviductal tissues of *Pmca4*^{-/-}, compared to WT (Fig. 5E, see also Fig. S1 in Supplementary data).

Identification of PMCA4 interacting partners in OVS and their interaction with PMCA1

Previous studies have shown that neuronal NOS (nNOS) and calcium/calmodulin-dependent serine kinase (CASK) interact with PMCA4 differently under capacitating and uncapsulating conditions in murine (Aravindan et al., 2012; Olli et al., 2018) and human (Andrews

et al., 2015) sperm. In order to investigate the presence of these PMCA4 interacting partners in OVS and to determine if they interact with PMCA1, we isolated OVS from WT females hormonally induced into estrus and probed their proteins via western blot analysis. In Fig. 6A, using testis as positive control, it was observed that both WT and *Pmca4*^{-/-} OVS carry CASK (100 kDa, membrane-associated form) and nNOS (155 kDa). We investigated if nNOS and CASK are interacting partners of PMCA1 in *Pmca4*^{-/-} OVS/OLF, as they are for PMCA4 in sperm, by performing co-immunoprecipitation assays. The results show that nNOS and CASK antibodies are able to co-immunoprecipitate



PMCA1 (Fig. 6B and C), while the IgG controls showed faint bands, indicating that PMCA1 associates with nNOS and CASK in OVS in the OLF.

In vitro uptake of enzymatically active PMCA1 and tyrosine-phosphorylated proteins after sperm–OVS co-incubation

Co-incubation assays were performed to investigate the potential delivery of PMCA1 from OVS/OLF to sperm, as previously shown for PMCA4 from female luminal fluids (Al-Dossary *et al.*, 2013, 2015). Flow cytometry revealed that PMCA1 in OLF was delivered to sperm following co-incubation with OLF. There was a 2-fold increase in the % of uncapacitated sperm in the region with the highest fluorescence intensity (FI) for PMCA1 following co-incubation with OLF (Fig. 7A (b)), compared to the PBS control (Fig. 7A (a)), while there was a >2-fold increase for capacitated sperm, compared to uncapacitated in OLF (Fig. 7A (c)). Therefore, capacitated sperm had the highest level of PMCA1, as also seen for the average data from three experiments (Fig. 7B) as well as from the frequency of cells with immuno-labeled topology (Fig. 7C). Figure 7B shows that the average frequency of sperm with the highest FI was significantly ($P < 0.05$) higher for uncapacitated sperm in OLF, compared to those in PBS. In OLF it was significantly higher ($P < 0.001$) in capacitated compared to uncapacitated. In corroborating the flow cytometric data, topology immunolabeling showed that PMCA1 uptake occurs on both the head and the flagellum where the protein is mostly localized before uptake (Fig. 7C (a, d)).

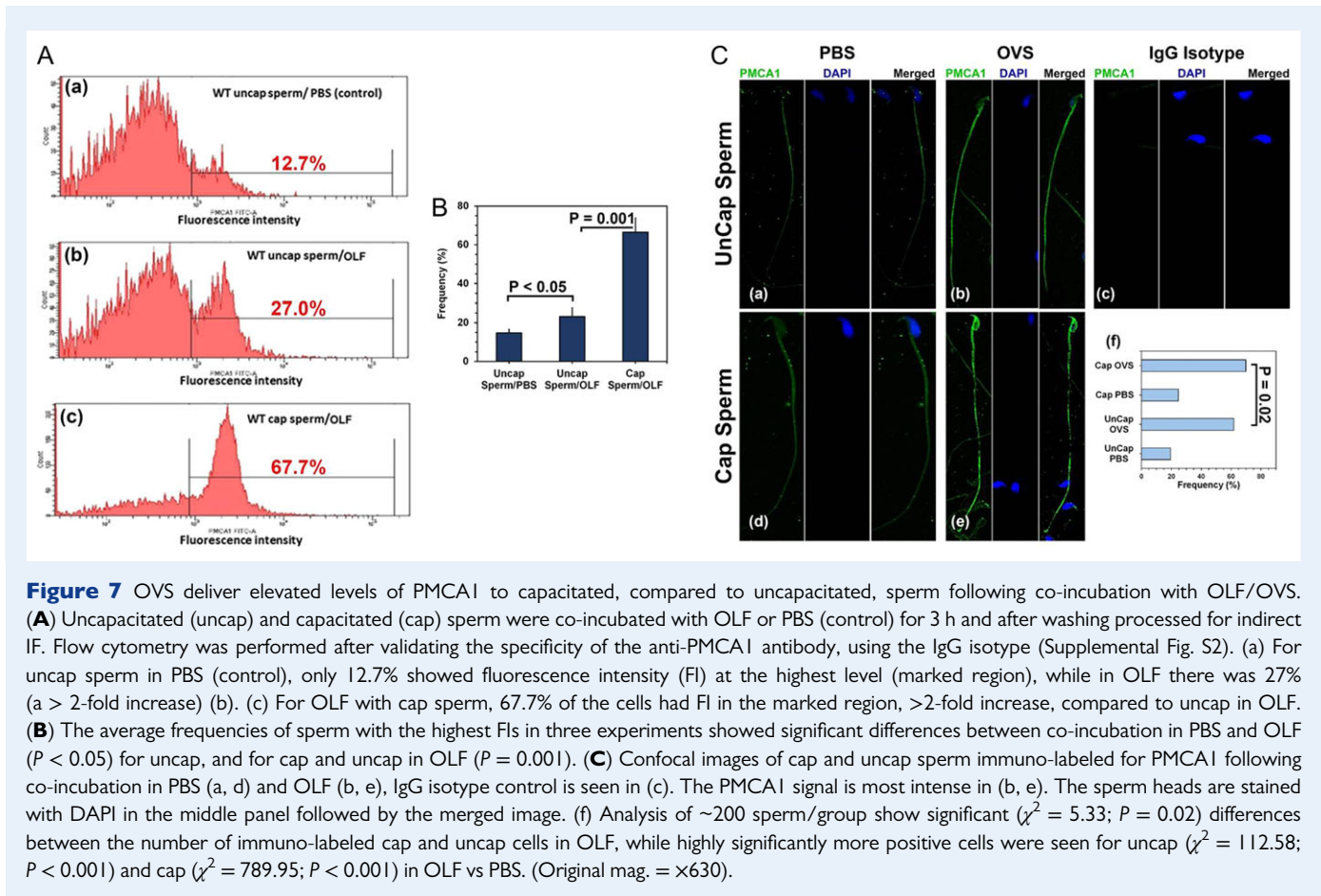
To investigate if the amount of surface PMCA1 revealed by flow cytometry could be a result of the removal of coating proteins or exposure of cryptic sites during the 3 h co-incubation, we performed

an experiment in which the co-incubation periods were 30 min, 90 min and 3 h and quantified the uptake of PMCA1 (as well as the HSC70 OVS biomarker), via western blot analysis. We also included two additional controls, sperm co-incubated in the supernatant (SUP) after removal of OVS from OLF and others co-incubated in capacitating medium (HTF) (Fig. 8). In Fig. 8A and B using β -actin as a loading control, we show significantly higher levels PMCA1 in sperm co-incubated in OVS compared to SUP at both 30 min ($P < 0.001$) and 3 h ($P < 0.01$) for capacitated and uncapacitated sperm. When sperm were co-incubated for 30 min, 90 min and 3 h there was a similar trend with OVS, compared to PBS, showing significantly ($P < 0.05$) higher levels of PMCA1 at all three time periods (Fig. 8C and D). Similarly, HSC70 was present in significantly ($P < 0.05$; $P < 0.01$) higher amounts after co-incubation of sperm with OVS compared to the controls (Fig. 8E), indicating its simultaneous delivery with PMCA1. Interestingly, at all three time periods, the levels of HSC70 in sperm co-incubated in HTF were only marginally detectable (Fig. 8E).

We have previously shown that sperm viability is unaffected after co-incubation with OVS: after ~3 h co-incubation with fluorescently labeled OVS, live sperm were immobilized and subjected to fluorescence recovery after photobleaching (FRAP) analysis to show that OVS are mobile in the plasma membrane (Al-Dossary *et al.*, 2015). To determine if the PMCA1s acquired by sperm from OVS are enzymatically active, we analyzed OVS from WT (containing PMCA1 and PMCA4) and *Pmca4*^{-/-} (only PMCA1 present) females and showed both to have Ca^{2+} -ATPase activity, with the level being significantly ($P = 0.03$) higher in the latter (Fig. 8F). Importantly, following co-incubation of sperm with OVS, the level of Ca^{2+} -ATPase activity was significantly ($P = 0.01$) elevated (Fig. 8F). Our results show that OVS contain and can deliver enzymatically active PMCA1 and PMCA4 to sperm.

Since protein tyrosine phosphorylation is known to stimulate sperm capacitation and is a marker of the process (Visconti *et al.*, 1995; Baker *et al.*, 2006), we examined the effect of co-incubation of sperm with OVS on sperm protein tyrosine phosphorylation. Western blot analysis showed that sperm protein tyrosine phosphorylation was increased after co-incubation of sperm with OVS for as short a period of 30 min when there was a gain of a prominent 55 kDa band, faintly seen with HTF (Fig. 9A). It also revealed that OVS carry tyrosine phosphorylated proteins in their cargo, including a 55 kDa band (Fig. 9B). A comparison of fresh and spent OVS that had been co-incubated with sperm for 15 and 90 min showed spent OVS to be missing two tyrosine phosphorylated bands (at ~180 kDa) that are present in the fresh samples.

To quantify sperm tyrosine phosphorylation levels, flow cytometry was performed following co-incubation of sperm with HTF (which supports capacitation), OVS or PBS (the OVS vehicle) for 2 h. FI increased for HTF and OVS, compared to that for the PBS control (Fig. 9C). The highest intensity was seen for sperm–OVS incubation which had an ~3-fold increase in the right peak channel shift, compared to PBS (259 vs 88; Fig. 9C). For HTF the increase was ~2-fold (162 vs 88). Protein tyrosine phosphorylation immunolabeling (Fig. 9D and E) showed a significantly ($\chi^2 = 19.27$; $P < 0.0001$) higher frequency of labeled sperm after co-incubation in OVS, compared to HTF; while HTF was significantly ($\chi^2 = 10.67$; $P < 0.001$) higher than PBS. The localization of the signal was only on the flagellum for sperm in PBS, while for those co-incubated in HTF and OVS the signal appeared on both the flagellum and the posterior head, but was far more intense for OVS (Fig. 9E). These data are consistent with the



western blot results indicating that OVS contribute markedly to increased levels of sperm tyrosine phosphorylation.

Discussion

OVS is evolutionarily conserved in humans and arise via the apocrine pathway

This study provides the first evidence of human OVS in the oviductal secretions. TEM revealed that these OVS were of both exosomal (<100 nm) and microvesicular (100–1000 nm) sizes, similar to those previously identified in the mouse (Al-Dossary et al., 2013, 2015) and bovine (Lopera-Vasquez et al., 2016), the other mammalian species studied to date. It is noteworthy that human OVS, characterized by the presence of the HSC70 biochemical marker, were shown to carry PMCA4 and eNOS which are fertility-modulating sperm proteins (Okunade et al., 2004; Schuh et al., 2004; Olli et al., 2018). These proteins are also present in human prostasomes which are able to deliver them to sperm (Andrews et al., 2015). Human OVS were also shown to carry PMCA1, a crucial housekeeping family member of PMCA4, which is ubiquitously expressed and leads to embryonic lethality in mice when deleted (Okunade et al., 2004). As demonstrated in this study, in mice OVS PMCA1 can compensate for PMCA4 in *Pmca4*^{-/-} and this is associated with female fertility. Thus, all the fertility-modulating proteins identified to date in the cargo of murine OVS appear to be conserved in human OVS.

EVs may arise via one of two processes: a pathway involving multi-vesicular bodies whose outer membrane fuses with the apical membrane of epithelial cells to release exosomes (They et al., 2002; Pisitkun et al., 2004); and the apocrine pathway in which blebs containing EVs dislodge from the apical membrane and enter the lumen where they release the EVs (Hermo and Jacks, 2002; Caballero et al., 2010). We investigated the biogenesis of OVS, by examining their location *in situ* in the murine oviduct. The presence of blebs containing EVs in the intraluminal compartment of oviductal sections provides evidence that OVS arise via the apocrine pathway. Interestingly, both microvesicular and exosomal OVS were shown to arise by this pathway which is also involved in the biogenesis of EVs in the male reproductive tract (Aumüller et al., 1999).

Expression and secretion of PMCAI in the murine female reproductive tract

To determine if PMCA1 compensates for PMCA4 in *Pmca4*^{-/-} females, accounting for their fertility, we studied PMCA1 expression in WT and KO female tissues (which appeared histologically normal), luminal fluids, and OVS. Using IF, we show that PMCA1 is expressed in the oviduct, uterus and vagina with the most intense staining in the oviduct. Notably, all the regions exhibited PMCA1 localization on the luminal side of the apical membrane of the epithelium, suggesting that PMCA1 is secreted into the lumens, similar to PMCA4 (Al-Dossary et al., 2013). Western blot analysis confirmed the presence of PMCA1 in female tissues and revealed similar expression levels in WT and

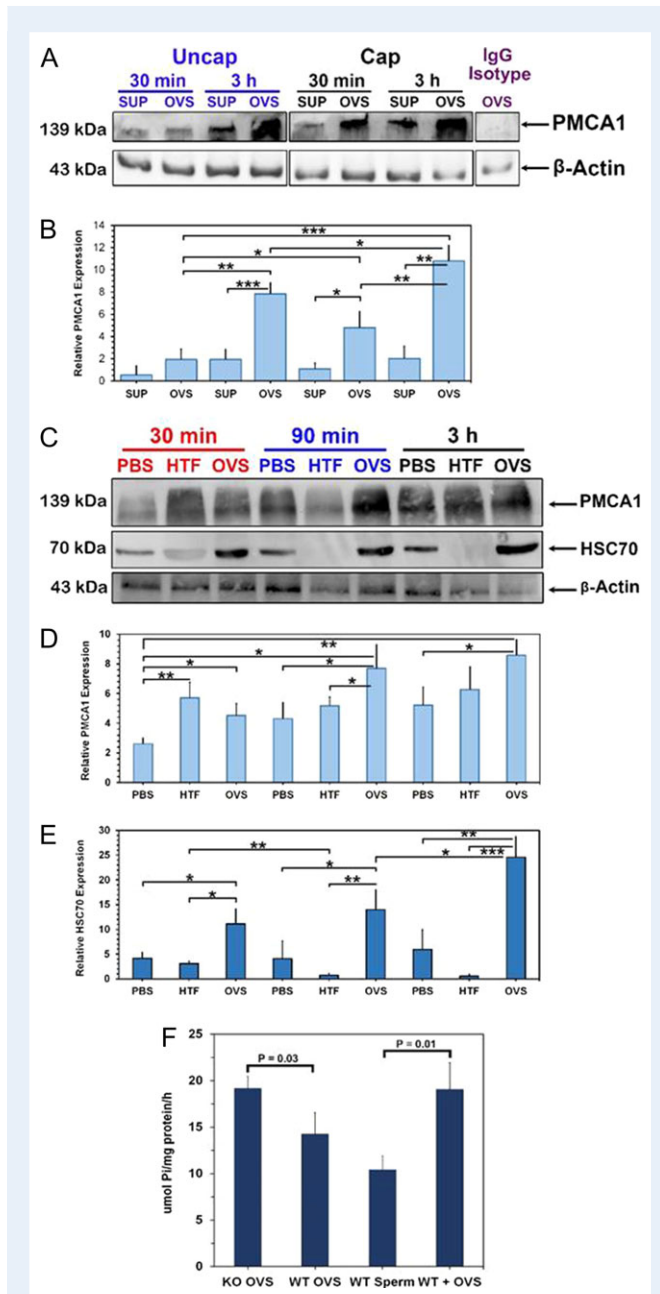


Figure 8 Quantitative western reveals that OVS deliver enzymatically active PMCA1 and HSC70 to sperm in significantly higher levels to capacitated, compared to uncapacitated ones. **(A)** Western blot of PMCA1 in proteins of uncapacitated (uncap) and capacitated (cap) sperm after co-incubation with OVS or oviductal luminal fluid (OLF) supernatant (SUP) for 30 min and 3 h shows the highest band intensities in cap sperm. The IgG isotype control was negative. The membrane was stripped and re-probed with β -actin, as a loading control. **(B)** One-way ANOVA and Student *t*-tests on the means of band intensities in (A) show significant differences for cap and uncap sperm in OVS compared to SUP for both time periods ($P < 0.001$, $P < 0.01$). **(C)** Western blot of PMCA1 and HSC70 levels after co-incubation of sperm with PBS, human tubal fluid (HTF), and OVS for 30 min, 90 min and 3 h show significantly elevated levels for OVS compared to PBS and HTF as seen in **(D)** and **(E)**. The levels of HSC70 for sperm in HTF was notably significantly lower than those in OVS and PBS.

Pmca4^{-/-}, as they were for testis. However, in natural cycling females OLF showed elevated levels of PMCA1 in *Pmca4*^{-/-} compared to WT. This provides support for the hypothesis that OVS PMCA1 compensates for PMCA4's loss in *Pmca4*^{-/-} females, as all the membrane proteins in OLF are carried on OVS (Al-Dossary *et al.*, 2013). The absence of upregulation of PMCA1 in epididymosomes of ELF is consistent with its absence in sperm and testis of *Pmca4*^{-/-} males where PMCA4's loss leads to infertility (Okunade *et al.*, 2004).

Natural cycling not only showed significantly elevated levels of OLF PMCA1 during estrus in *Pmca4*^{-/-}, but also revealed nulls to have a significant PMCA1 decrease during metestrus/diestrus stages when sperm are not present in the oviduct. This pattern of OLF PMCA1 expression in the *Pmca4*^{-/-}, not seen in the WT, mirrors that seen for OLF PMCA4 in WT females (Al-Dossary *et al.*, 2013), and argues that OVS PMCA1 is a true surrogate for OVS PMCA4 in nulls. The absence of a significant difference in the levels of PMCA1 in proestrus/estrus and metestrus/diestrus in WT suggests that PMCA1 plays no specific role in the WT's estrus cycle, underscoring the compensatory role of its upregulation in *Pmca4*^{-/-} OLF. This finding also indicates that PMCA1 and PMCA4 are not redundant isoforms, but have different functional profiles, as can be seen in the phenotypes generated when the genes are deleted (Okunade *et al.*, 2004).

The significant upregulation of PMCA1 in isolated OVS collected after hormonally induced estrus in *Pmca4*^{-/-} is consistent with the elevated levels of PMCA1 in the corresponding OLF, since transmembrane proteins are carried in the vesicular fraction of OLF (Al-Dossary *et al.*, 2013). *Pmca4*^{-/-} OVS were shown to be uniquely different from uterosomes which showed no increase of PMCA1. This finding also runs parallel to the significantly lower level of PMCA4 reported in the WT ULF, compared to OLF (Al-Dossary *et al.*, 2013), and highlights OVS PMCA1 as showing a uniquely compensatory role in *Pmca4*^{-/-}. Importantly, the finding that PMCA1 is upregulated in KO OVS, but not KO oviductal tissues, suggests that PMCA1 may be differentially expressed throughout the tissues with the higher levels in the apical luminal epithelial surface which secretes OVS. This would be consistent with the significant increase of *Pmca1* transcripts detected in KO tissues. Alternatively, PMCA1 levels may not be elevated in apical luminal epithelial surface, but PMCA1 may be selectively packaged in OVS. Selective packaging of the cargo in EVs has been reported under physiological (Belleannee *et al.*, 2013) as well as experimental (Aalberts *et al.*, 2012) and pathological (Palma *et al.*, 2012) conditions; although the process responsible for the enrichment is still unclear. However, the enrichment of PMCA1 in *Pmca4*^{-/-} OVS is likely to play a crucial role in maintaining Ca^{2+} homeostasis in oviductal sperm following capacitation, hyperactivation and the acrosome reaction all of which require Ca^{2+} influx, as proposed for PMCA4 (Al-Dossary *et al.*, 2013).

Quantification of the western blot data (B, D, E) represents the mean (\pm SEM, $n = 3$) of band intensities, using Image Lab 6.0 software. Significant levels are * <0.05 , ** <0.01 , *** <0.001 . **(F)** Mg^{2+} -dependent Ca^{2+} -ATPase assays of microsomes from OVS and cap sperm reveal that WT and KO OVS carry enzymatically active PMCA1/4 and that sperm-OVS (WT + OVS) co-incubation significantly increased the level of activity in sperm ($P = 0.01$). Activity in KO OVS was significantly ($P = 0.03$) higher than that in WT (\pm SEM, $n = 3$).

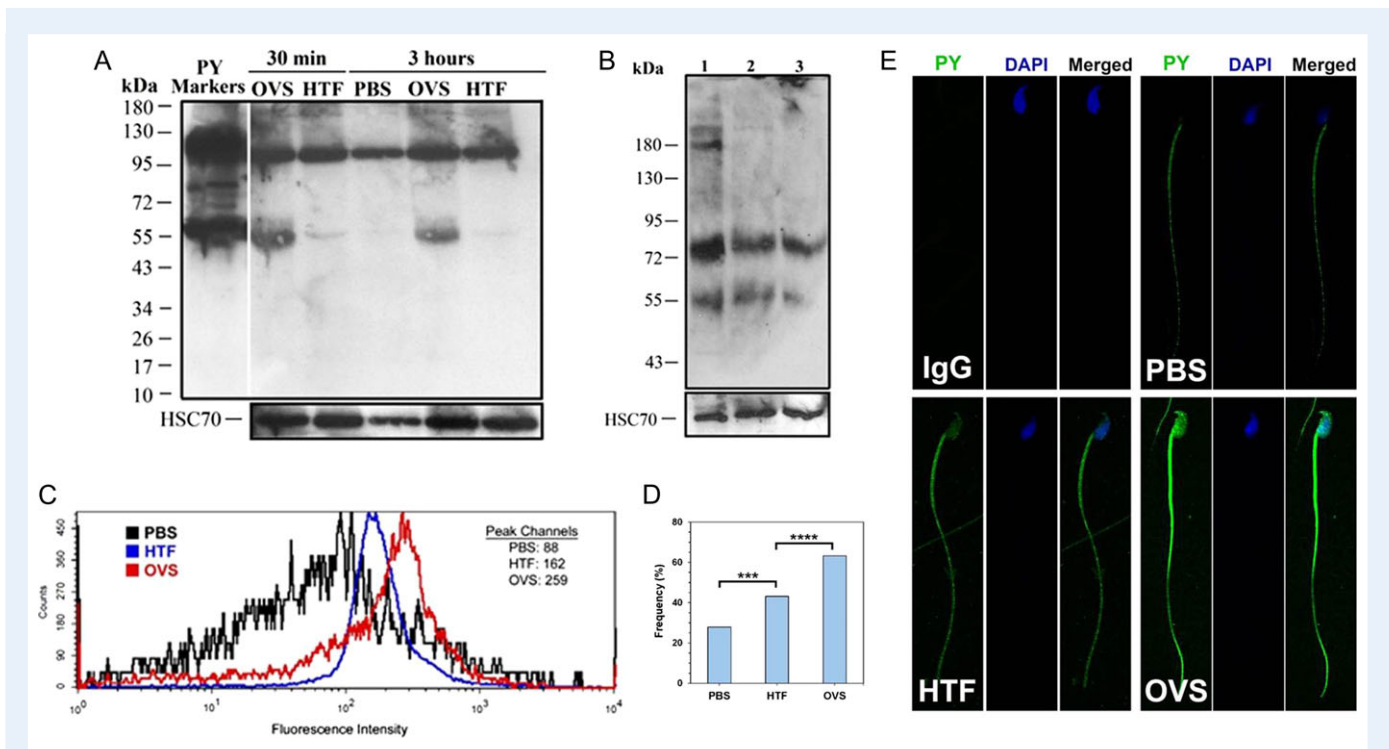


Figure 9 OVS carry tyrosine-phosphorylated proteins (PY) which are markedly increased in sperm following co-incubation with OVS. **(A)** Sperm were co-incubated with OVS re-constituted in PBS, or HTF capacitating medium, or PBS alone, for 30 min or 3 h. Proteins extracted from washed sperm were analyzed by western blot and membranes re-probed for HSC70. PY markers (first lane), positive control, and the usual 95 kDa sperm band are seen in all samples. The number and intensity of PY bands increased markedly in OVS samples, where there was a prominent 55 kDa band, faintly seen in HTF. The data are representative of four experiments. **(B)** Samples of OVS re-constituted in PBS were subjected to western blot analysis. Sample #1 was fresh (unused) and #2 and #3 were spent samples recovered after sperm-OVS co-incubation for 15 and 90 min, respectively. The amount of proteins loaded were 6.2 μ g (#1), 12.7 μ g (#2), and 12.9 μ g (#3). Sample #1 had at least four bands, while samples #2 and 3 had only two bands, documenting the presence of PY in OVS. **(C)** Flow cytometry showed the levels of PY in aliquots of sperm co-incubated with PBS, HTF and OVS re-constituted in PBS for 2 h. The graph shows a right peak shift in FI with peak channel values of 88 (PBS), 162 (HTF) and 259 (OVS), reflecting an increase in FI of PY in sperm following incubation in capacitating medium and more markedly after their interaction with OVS. The IgG control is seen in Supplemental Fig. S2. **(D, E)** Indirect IF shows the localization and uptake of PY in the sperm head and flagellum, with significantly higher numbers of immuno-labeled cells seen after co-incubation with OVS vs HTF ($\chi^2 = 19.27$; $P < 0.0001$) and HTF vs PBS ($\chi^2 = 10.67$; $P < 0.001$). For each treatment ~ 200 sperm were analyzed. The absence of a signal in the IgG isotype control (E) shows the specificity of the primary antibody (original mag. = $\times 630$).

It should be noted that PMCA1 is less efficient in its activity and is less stable than PMCA4 (Guerini et al., 2003). This may explain the 13-fold increase of PMCA1 in *Pmca4* KO OVS which might be necessary to compensate for the more efficient and stable PMCA4 in the oviduct where calcium extrusion is vital not only for the fertilizing sperm, but also for ciliary action in the oviductal epithelium. To our knowledge, this is the first report of a significant upregulation of a PMCA isoform (PMCA1) in the absence of another, and this is likely to have resulted partly from selective enrichment in its packaging in OVS, and partly from increased synthesis at pro/estrus. Increased PMCA1 synthesis at pro/estrus is likely to be under the control of estrogen, as suggested for PMCA4 (Al-Dossary et al., 2013).

Presence of PMCA4 interacting partners in OVS and their interaction with PMCA1

Recently, we showed that PMCA4 interacts with eNOS, nNOS and CASK in murine (Aravindan et al., 2012; Olli et al., 2018) and human

(Andrews et al., 2015) sperm. As these interacting partners are essential to maintain calcium homeostasis and to prevent nitric oxide toxicity in sperm and are delivered to them via prostasomes (Andrews et al., 2015), we investigated the presence of CASK and nNOS in murine OVS and show their presence in WT and *Pmca4*^{-/-} OVS where they co-immunoprecipitated with PMCA1. For *Pmca4*^{-/-}, the data suggested that nNOS was upregulated in both OVS and testis. While upregulation of OVS nNOS may ensure the presence of stoichiometric amounts for interaction with upregulated PMCA1, the upregulation in the testis where PMCA1 levels are unaltered in *Pmca4*^{-/-} (Okunade et al., 2004) is unexplained. Co-immunoprecipitation of the proteins indicates that they are in a complex in OVS, as they are with PMCA4 in epididymosomes (Martin-DeLeon, 2015) which also relay them to sperm during epididymal maturation (Patel et al., 2013; Martin-DeLeon, 2015). Importantly, this finding further reveals that PMCA1 in its compensatory role in *Pmca4*^{-/-} OVS acts as a true surrogate of PMCA4, in a complex that regulates nitric oxide levels and Ca²⁺ homeostasis.

OVS transfer enzymatically active PMCA4 and tyrosine phosphorylated proteins to sperm

Co-incubation assays reveal that PMCA1, like PMCA4 (Al-Dossary *et al.*, 2013, 2015), can be delivered to sperm by OVS/OLF. Elevated levels of HSC70, an exosomal marker, accompanied those of PMCA1, consistent with exosomal cargo delivery. The amount of PMCA1 delivered was significantly higher in capacitated, compared to uncapacitated, sperm in all three approaches: flow cytometry, quantitative western blot and the frequency of sperm with immuno-labeled topology. As capacitated sperm have increased membrane fluidity (Brouwers *et al.*, 2011; Boerke *et al.*, 2013), this could increase OVS cargo delivery which was shown to occur via membrane fusion (Al-Dossary *et al.*, 2015). Alternatively, the increase in PMCA1 uptake in capacitated sperm may represent its acquisition on both the plasma membrane and the inner acrosomal membrane (IAM), as PMCA4 has been shown to reside on both (Al-Dossary *et al.*, 2015). The IAM in capacitated sperm is likely to become exposed in a subpopulation of sperm that acrosome-react, and could acquire additional PMCA1 from OVS/OLF during co-incubation. In this vein, the finding that sperm co-incubated in capacitating medium (HTF) showed only marginally detectable levels of HSC70 may be explained by loss of this soluble membrane-associated protein in the subpopulation of sperm that acrosome-react. Whatever may be the basis for the increased uptake of PMCA1 in capacitated cap sperm, their association or correlation is of functional significance. Since the PMCA4 delivered to sperm from OVS were shown to be enzymatically active they would serve to maintain Ca^{2+} homeostasis after influxes associated with capacitation. Interestingly, *Pmca4*^{-/-} OVS were shown to have significantly increased enzyme activity, compared to WT. This is consistent with the significant increase in PMCA1 expression observed, and may be required to compensate for the more stable and efficient PMCA4 (Guerini *et al.*, 2003).

Finally, the increased expression and sperm uptake of OVS PMCA1 associated with capacitation and fertility in *Pmca4*^{-/-} prompted us to determine the effect of sperm–OVS interaction on tyrosine phosphorylation levels, a signature of capacitation (Visconti *et al.*, 1995; Baker *et al.*, 2006). Our results clearly show increased tyrosine phosphorylation with sperm–OVS interaction. Similar findings were obtained for human sperm (data not shown). Note that because of the prolonged period (3 h instead of 90 min sperm incubation) in HTF, the capacitating medium, the capacitation-associated increase in phosphorylation was diminished in the western blot data. Importantly, tyrosine phosphorylated proteins were shown to be present in OVS which displayed heterogeneity with respect to cargo constituents, as the two samples (spent or used) had two bands compared to at least four in the fresh sample. Heterogeneity is consistent with the report that all OVS do not carry the same cargo (Al-Dossary *et al.*, 2015) and the notion that used samples should be less heterogeneous in the smaller population of OVS remaining after cargo delivery.

The increased protein tyrosine phosphorylation associated with OVS delivery is consistent with a recent report showing that fusion of uterosome-like vesicles with human sperm prompt capacitation by increasing protein tyrosine phosphorylation levels (Franchi *et al.*, 2016). Our data indicate that OVS carry and deliver a subset of murine sperm tyrosine-phosphorylated proteins to sperm, although they might also

deliver proteins that activate signal transduction pathways involved in producing these proteins. It is known that FER is the tyrosine kinase responsible for capacitation-associated increase in tyrosine phosphorylation in murine sperm (Alvau *et al.*, 2016). The recent finding that mice missing FER (due to a targeted kinase-inactivating mutation of *Fer*) have significantly reduced levels of tyrosine phosphorylation in capacitated sperm and reduced *in vitro* fertilization rates, yet they are fertile (Alvau *et al.*, 2016), suggests that OVS deliver these proteins to sperm *in vivo* to maintain fertility. These observations strongly support OVS' role in the delivery of tyrosine phosphorylated proteins to sperm during capacitation and suggest that these proteins are required for both *in vivo* and *in vitro* fertilization in the mouse.

Overall, the data from both WT and *Pmca4*^{-/-} females reveal that OVS play a pivotal role in capacitation and fertility. As OVS are understudied, further investigations are expected to reveal the extent of their cargo composition, and provide an understanding of their interactions with oocytes and embryos (Machtinger *et al.*, 2016), as well as the implications for human infertility treatment and exosome diagnostics and therapeutics.

Conclusions

In this study we show that OVS are evolutionarily conserved in humans and arise from the apocrine pathway. They carry and can deliver to sperm important fertility-modulating proteins, including PMCA4 and PMCA1 which are Ca^{2+} efflux pumps with different functional profiles during the murine estrus cycle. While the levels of OVS PMCA1 are not different during the cycle in WT females, *Pmca4*^{-/-} carry significantly elevated proestrus/estrus levels, mimicking the expression pattern of OVS PMCA4 and acting as its surrogate. This upregulation of PMCA1 in OVS is not seen in other reproductive EVs. As increased PMCA1 levels were not detected in the *Pmca4*^{-/-} parental oviductal tissues, despite an increase in *Pmca1* transcript, selective packaging of the protein in OVS is partly likely to occur. While *Pmca4*^{-/-} males are infertile, the compensatory role of OVS PMCA1 in the absence of PMCA4 explains the fertility of females. Importantly protein tyrosine phosphorylation, a key intracellular event in capacitation, is enhanced by OVS cargo delivery to sperm. Together, these observations underscore OVS' pivotal role in fertility. They also have implications for human infertility treatment and exosome diagnostics and therapeutics.

Supplementary data

Supplementary data are available at *Molecular Human Reproduction* online.

Acknowledgements

Thanks are extended to Michael Moore and Jeffrey Caplan of the Bioimaging Center at Delaware Biotechnology Institute for assistance with confocal microscopy, and the rendering of the tomographic images, respectively. Thanks are also due to Dr John McDonald for help with statistics. We are grateful for Tori Mallardi's assistance with the western blots.

Authors' roles

The experiments were designed by P.B. and P.A.M.-D. and the majority of the studies (westerns, indirect immunofluorescence, confocal microscopy, co-immunoprecipitation) were performed by P.B. and submitted in partial fulfillment for the requirements of the Master's degree. Z.F. performed the flow cytometric analysis, the quantitative western blots and immunofluorescence after *in vitro* uptake of PMCA1 and the qRT-PCR. K.L. performed the protein tyrosine phosphorylation studies, and the characterization of the human extracellular vesicles. A.A.A. performed the Ca²⁺-ATPase activity, and D.S.G assisted with the flow cytometry analysis. The article was written by P.B. and P.A.M.-D.

Funding

National Institute of Health (5P20RR015588) and (RO3HD073523).

Conflict of interest

No competing interests declared.

References

- Aalberts M, van Dissel-Emiliani FM, van Adrichem NP, van Wijnen M, Wauben MH, Stout TA, Stoorvogel W. Identification of distinct populations of prostasomes that differentially express prostate stem cell antigen, annexin A1, and GLIPR2 in humans. *Biol Reprod* 2012;**86**:82.
- Adeoya-Osiguwa SA, Fraser LR. Evidence for Ca²⁺-dependent ATPase activity, stimulated by decapacitation factor and calmodulin, in mouse sperm. *Mol Reprod Dev* 1996;**44**:111–120.
- Al-Dossary AA, Bathala P, Caplan JL, Martin-DeLeon PA. Oviductosome-sperm membrane interaction in cargo delivery: detection of fusion and underlying molecular players using 3D super-resolution structured illumination microscopy (SR-SIM). *J Biol Chem* 2015;**290**:17710–17723.
- Al-Dossary AA, Strehler EE, Martin-DeLeon PA. Expression and secretion of plasma membrane Ca²⁺-ATPase 4a (PMCA4a) during murine estrus: association with oviductal exosomes and uptake in sperm. *PLoS One* 2013;**8**:e80181.
- Alvau A, Battistone MA, Gervasi MG, Navarrete FA, Xu X, Sanchez-Cardenas C, De la Vega-Beltran JL, Da Ros VG, Greer PA, Darszon A et al. The tyrosine kinase FER is responsible for the capacitation-associated increase in tyrosine phosphorylation in murine sperm. *Development* 2016;**143**:2325–2333.
- Andrews RE, Galileo DS, Martin-DeLeon PA. Plasma membrane Ca²⁺-ATPase 4: interaction with constitutive nitric oxide synthases in human sperm and prostasomes which carry Ca²⁺/CaM-dependent serine kinase. *Mol Hum Reprod* 2015;**21**:832–843.
- Aravindan RG, Fomin VP, Naik UP, Modelski MJ, Naik MU, Galileo DS, Duncan RL, Martin-DeLeon PA. CASK interacts with PMCA4b and JAM-A on the mouse sperm flagellum to regulate Ca²⁺ homeostasis and motility. *J Cell Physiol* 2012;**227**:3138–3150.
- Aumüller G, Wilhelm B, Seitz J. Apocrine secretion-fact or artifact? *Ann Anat* 1999;**181**:437–446.
- Austin CR. The capacitation of the mammalian sperm. *Nature* 1952;**170**:326.
- Baker MA, Hetherington L, Aitken RJ. Identification of SRC as a key PKA-stimulated tyrosine kinase involved in the capacitation-associated hyperactivation of murine spermatozoa. *J Cell Sci* 2006;**119**:3182–3192.
- Belleannee C, Calvo E, Caballero J, Sullivan R. Epididymosomes convey different repertoires of microRNAs throughout the bovine epididymis. *Biol Reprod* 2013;**89**:30.
- Boerke A, Brouwers JF, Olkkonen VM, van de Lest CH, Sostaric E, Schoevers EJ, Helms JB, Gadella BM. Involvement of bicarbonate-induced radical signaling in oxysterol formation and sterol depletion of capacitating mammalian sperm during *in vitro* fertilization. *Biol Reprod* 2013;**88**:21.
- Brouwers JF, Boerke A, Silva PF, Garcia-Gil N, van Gestel RA, Helms JB, van de Lest CH, Gadella BM. Mass spectrometric detection of cholesterol oxidation in bovine sperm. *Biol Reprod* 2011;**85**:128–136.
- Byers SL, Wiles MV, Dunn SL, Taft RA. Mouse estrous cycle identification tool and images. *PLoS One* 2012;**7**:e35538.
- Caballero J, Frenette G, Sullivan R. Post testicular sperm maturational changes in the bull: important role of the epididymosomes and prostasomes. *Vet Med Int* 2010;**2011**:757194.
- Chang MC. Development of fertilizing capacity of rabbit spermatozoa in the uterus. *Nature* 1955;**175**:1036–1037.
- Chen H, Griffiths G, Galileo DS, Martin-DeLeon PA. Epididymal SPAMI is a marker for sperm maturation in the mouse. *Biol Reprod* 2006;**74**:923–930.
- Franchi A, Cubilla M, Guidobaldi HA, Bravo AA, Giojalas LC. Uterosome-like vesicles prompt human sperm fertilizing capability. *Mol Hum Reprod* 2016;**22**:833–841.
- Ghersevich S, Massa E, Zumoffen C. Oviductal secretion and gamete interaction. *Reproduction* 2015;**149**:R1–R14.
- Griffiths GS, Galileo DS, Reese K, Martin-DeLeon PA. Investigating the role of murine epididymosomes and uterosomes in GPI-linked protein transfer to sperm using SPAMI as a model. *Mol Reprod Dev* 2008;**75**:1627–1636.
- Guerni D, Pan B, Carafoli E. Expression, purification, and characterization of isoform I of the plasma membrane Ca²⁺ pump: focus on calpain sensitivity. *J Biol Chem* 2003;**278**:38141–38148.
- Hermo L, Jacks D. Nature's ingenuity: bypassing the classical secretory route via apocrine secretion. *Mol Reprod Dev* 2002;**63**:394–410.
- Kosk-Kosicka D. Measurement of Ca²⁺-ATPase activity in PMCA and SERCA. In: Lambert DG (ed). *Calcium Signaling Protocols*. Totowa, New Jersey: Humana Press, 1999:343–359.
- Kremer JR, Mastronarde DN, McIntosh JR. Computer visualization of three-dimensional image data using IMOD. *J Struct Biol* 1996;**116**:71–76.
- Lopera-Vasquez R, Hamdi M, Fernandez-Fuertes B, Maillou V, Beltran-Brena P, Calle A, Redruello A, Lopez-Martin S, Gutierrez-Adan A, Yanez-Mo M et al. Extracellular vesicles from BOEC in *in vitro* embryo development and quality. *PLoS One* 2016;**11**:e0148083.
- Machtinger R, Laurent LC, Baccarelli AA. Extracellular vesicles: roles in gamete maturation, fertilization and embryo implantation. *Hum Reprod Update* 2016;**22**:182–193.
- Martin-DeLeon PA. Epididymosomes: transfer of fertility-modulating proteins to the sperm surface. *Asian J Androl* 2015;**17**:720–725.
- Martin-DeLeon PA. Extracellular vesicles in the reproductive tracts: roles in sperm maturation and function. In: Meyer A (ed). *Exosomes: Biogenesis, Therapeutic Applications and Emerging Research*. Nova Biomedical, New York: Nova Science Publishers, 2016:79–100.
- Okunade GW, Miller ML, Pyne GJ, Sutliff RL, O'Connor KT, Neumann JC, Andringa A, Miller DA, Prasad V, Doetschman T et al. Targeted ablation of plasma membrane Ca²⁺-ATPase (PMCA) 1 and 4 indicates a major house-keeping function for PMCA1 and a critical role in hyperactivated sperm motility and male fertility for PMCA4. *J Biol Chem* 2004;**279**:33742–33750.
- Olli KE, Li K, Galileo DS, Martin-DeLeon PA. Plasma membrane calcium ATPase 4 (PMCA4) co-ordinates calcium and nitric oxide signaling in regulating murine sperm functional activity. *J Cell Physiol* 2018;**233**:11–22.
- Palma J, Yaddanapudi SC, Pigati L, Havens MA, Jeong S, Weiner GA, Weimer KM, Stern B, Hastings ML, Duelli DM. MicroRNAs are exported from malignant cells in customized particles. *Nucleic Acids Res* 2012;**40**:9125–9138.

- Patel R, Al-Dossary AA, Stabley DL, Barone C, Galileo DS, Strehler EE, Martin-DeLeon PA. Plasma membrane Ca²⁺-ATPase 4 in murine epididymis: secretion of splice variants in the luminal fluid and a role in sperm maturation. *Biol Reprod* 2013;**89**:6.
- Pisitkun T, Shen RF, Knepper MA. Identification and proteomic profiling of exosomes in human urine. *Proc Natl Acad Sci USA* 2004;**101**:13368–13373.
- Post H, Schwarz A, Brandenburger T, Aumuller G, Wilhelm B. Arrangement of PMCA4 in bovine sperm membrane fractions. *Int J Androl* 2010;**33**:775–783.
- Rasband WS. ImageJ, U. S. National Institutes of Health. 1997–2016. Bethesda, Maryland, USA, <http://imagej.nih.gov/ij/>.
- Reynolds ES. The use of lead citrate at high pH as an electron-opaque stain in electron microscopy. *J Cell Biol* 1963;**17**:208–212.
- Rozen S, Skaletsky H. Primer 3 on the WWW for general users and for biologist programmers. *Methods Mol Biol* 2000;**132**:365–386.
- Schuh K, Cartwright EJ, Jankevics E, Bundschu K, Liebermann J, Williams JC, Armesilla AL, Emerson M, Oceandy D, Knobeloch KP et al. Plasma membrane Ca²⁺ ATPase 4 is required for sperm motility and male fertility. *J Biol Chem* 2004;**279**:28220–28226.
- Simons M, Raposo G. Exosomes: vesicular carriers for intercellular communication. *Curr Opin Cell Biol* 2009;**21**:575–581.
- Strehler EE, Filoteo AG, Penniston JT, Caride AJ. Plasma-membrane Ca(2+) pumps: structural diversity as the basis for functional versatility. *Biochem Soc Trans* 2007;**35**:919–922.
- Thery C, Ostrowski M, Segura E. Membrane vesicles as conveyors of immune responses. *Nat Rev Immunol* 2009;**9**:581–593.
- Thery C, Zitvogel L, Amigorena S. Exosomes: composition, biogenesis and function. *Nat Rev Immunol* 2002;**2**:569–579.
- Visconti PE, Bailey JL, Moore GD, Pan D, Olds-Clarke P, Kopf GS. Capacitation of mouse sperm II. Protein tyrosine phosphorylation and capacitation are regulated by a cAMP-dependent pathway. *Development* 1995;**121**:1139–1150.
- Wennemuth G, Babcock DF, Hille B. Calcium clearance mechanisms of mouse sperm. *J Gen Physiol* 2003;**122**:115–128.